Gazi University Journal of Science
GU J Sci
24(2):329-339 (2011)

GUJS
www.gujs.org

Performance Comparison of Residual Control Charts for Trend Stationary First Order Autoregressive Processes

Aslan Deniz KARAOGLAN[1,♠], Gunhan Mirac BAYHAN[2]

[1]*Department of Industrial Engineering, Balikesir University, Cagis Campus, 10145, Balikesir-Turkey.*
[2]*Department of Industrial Engineering, Dokuz Eylul University, Tinaztepe Campus, 35160, Izmir-Turkey.*

Received:12.10.2010 Revised: 22.11.2010 Accepted: 23.11.2010

ABSTRACT

Data sets collected from industrial processes may have both a particular type of trend and correlation among adjacent observations (autocorrelation). Existing statistical control charts may individually cope with autocorrelated or trending data. Applying the Shewhart, EWMA, CUSUM, or GMA charts to the uncorrelated residuals of an appropriate time series model for a process is a primary method to deal with autocorrelated process data. In the relevant literature, there exists no study that shows how these charts' performances change by the addition of a particular type of trend in autocorrelated data. In the present paper, average run lengths of these charts are computed; first, for autocorrelated data which does not include an increasing linear trend, and second, for autocorrelated data which includes an increasing linear trend. It is assumed that stationary AR(1) model and trend stationary first order autoregressive (trend AR(1) for short) model, respectively, are suitable models for the test data. ARL performances are compared within the charts and among the charts. Comparisons are made for different magnitudes of the process mean shift and various levels of autocorrelation.

Keywords: *statistical process control, autocorrelation, linear trend, trend AR(1).*

1. INTRODUCTION

Since the first control chart has been proposed by Shewhart in 1931, lots of charts have been developed and then improved to use for different process data. In its basics form, a control chart compares process observations with a pair of control limits. The standard assumptions that are usually cited in justifying the use of control charts are that the data generated by the in-control process are normally and independently distributed by mean of μ and standard deviation of σ [1]. However the independency assumption is not realistic in practice. The most frequently reported effect on control charts of violating such assumptions is the erroneous assignment of the control limits. In 1995, Alwan and Roberts showed that about 85% of a sample of 235 control chart applications displayed incorrect control limits [2]. More than half of these displacements were due to violation of the independence assumption, that is, due to serial correlation in the data. However, many processes such as those found in refinery operations, smelting operations, wood product manufacturing, waste-water processing and the operation of nuclear reactors have been shown to have autocorrelated observations.

When there is significant autocorrelation in a process, traditional control charts with *iid* (independent and identically distributed) assumption will be ineffective. In addition to various control charts developed for monitoring autocorrelated processes, three general approaches are recommended; (i) fit ARIMA model to data then apply traditional control charts such as Shewhart, CUSUM, EWMA to process residuals, (ii) monitor the autocorrelated observations by modifying the standard control limits to account for the autocorrelation (iii) eliminate the autocorrelation by using an engineering controller [1].

When applying traditional charts to residuals, forecast errors, namely residuals, are assumed to be statistically uncorrelated. An appropriate time series model is fitted to the autocorrelated data and the residuals are plotted in a control chart. For this reason all of the well-known control schemes can be transformed to the residual control schemes. The main advantage of a residual chart is that it can be applied to any autocorrelated data whether the process is stationary or not. When the literature is reviewed for 1997-2010 year range, it is clearly observed that the following studies are remarkable. In 1997, Kramer & Schmid [3] discussed the application of the Shewhart chart to residuals of

♠Corresponding author, e-mail: deniz@balikesir.edu.tr

AR(1) process and in the same year Reynolds & Lu [4] compared performances of two different types of EWMA control charts for residuals of AR(1) process. Yang & Makis [5] compared the performances of Shewhart, CUSUM, EWMA charts for the residuals of AR(1) process. Zhang [6] remarked that the detection capability of an *x* residual chart was poor for small mean shifts compared to the traditional *x* chart, EWMA, and CUSUM charts for AR(2) process. Two years later Lu & Reynolds [7] compared the performances of EWMA control chart based on the residuals from the forecast values of AR(1) process and EWMA control chart based on the original observations. Luceno & Box [8] studied the one-sided CUSUM chart. Rao et al. [9] focused on the integral equation approach for computing the ARL for CUSUM control charts for AR(1) process. They studied the ARL performance versus length of the sampling interval between consecutive observations for residuals of AR(1) process. Jiang et al. [10] proposed proportional integral derivative (PID) charts for residuals of ARMA(1,1) process. Kacker & Zhang [11] studied the run length performance of Shewhart $\bar{x}$ for residuals of IMA(λ,σ) processes. Shu et al. [12] proposed a CUSUM-triggered Cuscore chart to reduce the mismatch between the detector and fault signature. A variation to the CUSUM-triggered Cuscore chart that uses a GLRT to estimate the mean shift time of occurrence is also discussed. They used ARMA(1,1) process to test the performance of proposed chart. It is shown that the triggered Cuscore chart performs better than the standard Cuscore chart and the residual-based CUSUM chart. Ben-Gal et al. [13] presented context-based SPC (CSPC) methodology for state-dependent discrete-valued data generated by a finite memory source and tested the performance of this new modified chart for AR(1), AR(2), MA(1) processes. Snoussi et al. [14] studied on residuals for short run autocorrelated data of autocorrelated process. They compared the performances of Shewhart $\bar{x}$, CUSUM, and EWMA control charts for residuals of AR(1) process. They also compared the performances of CUSUM and EWMA control charts with Q statistics (EWMA Q chart and CUSUM Q chart) for residuals of AR(1) process. Kim et al. [15] considered a CUSUM process as their monitoring statistic that is a bit different than that of Johnson & Bagshaw (1974), and they approximate this CUSUM process by a Brownian motion process. Noorossana & Vaghefi [16] investigated the effect of autocorrelation on performance of the MCUSUM control chart. Triantafyllopoulos [17] has developed a new multivariate control chart based on Bayes' factors. This control chart is specifically aimed at multivariate autocorrelated and serially correlated processes and tested for AR(1) process. Yang & Yang [18] considered the problem of monitoring the mean of a quality characteristic *x* on the first process step and the mean of a quality characteristic *y* on the second process step, in which the observations *x* can be modeled as an AR(1) model and observations *y* can be modeled as a transfer function of *x* since the state of the second process step is dependent on the state of the first process step. To effectively distinguish and maintain the state of the two dependent process steps, the Shewhart control chart of residual and the cause selecting chart (CSC) are proposed. They showed that the proposed control charts are much better than the misused Hotelling T^2 control chart and the individual shewhart chart. Ghourabi & Limam [19] proposed a new method of residual process control, the Pattern Chart and tested this new chart for AR(1) process and compared its ARL values with SCC chart. Costa & Claro [20] considered the double sampling (DS) $\bar{x}$ control chart for monitoring processes in which the observations can be represented as ARMA(1,1) model. Zou et al. [21] suggested using a variable sampling scheme at fixed times (VSIFT) to enhance the efficiency of the $\bar{x}$ control chart for the autocorrelated data. Two charts are under consideration, that is, the VSIFT $\bar{x}$ and variable sampling rate with sampling at fixed times (VSRFT $\bar{x}$) charts. These two charts are called $\bar{x}$-VSFT charts. The authors used AR(1) model as representative model for their study. An integration equation method combined with a Markov process model was developed to study the performance of these charts. Sheu & Lu [22] examined a GWMA with a time-varying control chart for monitoring the mean of a process based on AR(1) process and they compared ARL performance of GWMA and EWMA charts. Weiss & Testik [23] investigated the CUSUM control chart for monitoring autocorrelated processes of counts modeled by a Poisson integer-valued autoregressive model of order 1 (Poisson INAR(1)). Knoth et al. [24] discussed the impact of autocorrelation on the probability of misleading signals (PMS) of simultaneous Shewhart and EWMA residual schemes for the mean and variance of a AR(1) process.

Use of a residual chart has the advantage that it can be applied to any autocorrelated data even if the data from a nonstationary process. It needs time series modeling efforts [25]. Although the residual charts have some advantages by using them for autocorrelated processes, there are some problems due to the detection capability of the residual chart. Harris & Ross [26] recognized that the CUSUM control chart and EWMA control chart for the residuals from a first-order autoregressive (AR(1)) process may have poor capability to detect the process mean shift. Wardell et al. [27] showed that Shewhart charts are not completely robust to deviations from the assumption of process randomness; namely when observations are correlated. EWMA chart is very good at detecting small shifts, and performs well for large shifts at only the case when the autoregressive parameter is negative and the moving average parameter is positive. No other chart is obviously dominant under every condition. They showed that when the processes were positively autocorrelated (at the first lag), the residual chart did not perform very well. Zhang [28] also studied on detection capability of residual chart for autocorrelated data. In his study, Zhang defined a measure of the detection capability of the residual *x*-chart for the general stationary process and showed that the detection capability of a residual chart for AR(2) process was small compared to the detection capability of the *x* chart. One of the most important disadvantages of residual charts is that the time series modeling knowledge is needed for constructing the ARIMA model and some residual charts which based on two valid time series models signal differently.

In addition to autocorrelation, some types of industrial processes such as chemical processes also exhibit a particular kind of trend behavior. In chemical processes linear trend often occurs because of settling or separation of the components of a mixture. Such process data is usually modeled by a trend AR(1) model. Peroxide values of vegetable oil, cement production and etc. (see [29] and [30] for examples from industry) shows trend and also autocorrelation because of the nature of process. In such processes, there is varying (rather than a constant) average, and it is assumed that the values of the dependent variable are linearly (causally) related with the values of the independent variable. In this study, we want to compare performances of Shewhart, CUSUM, EWMA and GMA residual charts for trend AR(1) process. In the relevant literature, there exists no study that shows how these charts' performances change by the addition of a particular type of trend in autocorrelated data. Average run length (ARL) is used as performance criterion. ARL is defined as the number of observations that must be plotted before a point indicates an out-of-control condition. For a desired chart when the process has no mean shift the ARL should be large, and when a mean shift occurs the ARL should be small to indicate the occurrence of the mean shift quickly [25]. In the present paper, average run lengths of these charts are computed; first, for autocorrelated data which does not include an increasing linear trend, and second, for autocorrelated data which includes an increasing linear trend. It is assumed that stationary AR(1) model and trend stationary first order autoregressive (trend AR(1) for short) model, respectively, are suitable models for the test data. ARL performances are compared within the charts and among the charts. Comparisons are made for different magnitudes of the process mean shift and various levels of autocorrelation.

Rest of the paper is organized as follows. Next section describes required steps for constructing the residual charts under consideration. In Section 3, trend AR(1) model is described. Comparison between the residual charts' performances for AR(1) and trend AR(1) processes is given in Section 4. Conclusions are pointed out in Section 5.

2. CONTROL CHARTS FOR RESIDUALS

2.1. The Shewhart Chart

The Shewhart $\bar{x}$ and $\bar{R}$ chart which is the basis for many control charts is very simple and easy to use. If x_i are sample of size n, then the average of this sample is $\bar{x}$ and we know that $\bar{x}$ is normally distributed with mean μ and standard deviation $\sigma_{\bar{x}}$, where $\sigma_{\bar{x}} = \sigma / \sqrt{n}$. Then the best estimator of μ, the process average, is the grand average, say $\bar{\bar{x}}$. Then the center line (CL), upper control limit (UCL), and lower control limit (LCL) of the Shewhart $\bar{x}$ and R chart for the 3 standard deviations from the center-line are given below in Equation (1-3) respectively [1]:

$$UCL = \bar{\bar{x}} + 3\frac{\sigma}{\sqrt{n}} \quad (1)$$

$$CL = \bar{\bar{x}} \quad (2)$$

$$LCL = \bar{\bar{x}} - 3\frac{\sigma}{\sqrt{n}} \quad (3)$$

Where $\bar{\bar{x}} = (\bar{x}_1 + \bar{x}_2 + ... + \bar{x}_m) / m$, $\bar{x} = (x_1 + x_2 + ... + x_n) / n$, $\hat{\sigma} = \bar{R} / d_2$, $R = x_{\max} - x_{\min}$ and $\bar{R} = (R_1 + R_2 + ... + R_m) / m$.

If the production rate is too slow to allow sample sizes greater than one then individual measurements are used. For the control chart for individual measurements, the parameters are

$$UCL = \bar{x} + 3\frac{\overline{MR}}{d_2} \quad (4)$$

$$CL = \bar{x} \quad (5)$$

$$LCL = \bar{x} - 3\frac{\overline{MR}}{d_2} \quad (6)$$

where $\overline{MR}$ is the average moving range and MR is the range between consecutive observations [1].

If the observations are autocorrelated, the formulations are modified by using $\{e_t\}$ instead of $\{x_t\}$. For residual charts, the residual e_t from a time series model of $\{x_t\}$ is defined as

$$e_i = x_t - \hat{x}_t \quad (7)$$

where $\hat{x}_t$ is the prediction of $\{x_t\}$ from the time series model at time t. Various residual charts are constructed based on e_t depending on the traditional charts used. For a Shewhart residual chart the chart is constructed by charting e_t instead of $\{x_t\}$. Also the CUSUM residual, EWMA residual and GMA residual charts are constructed by applying traditional CUSUM, EWMA and GMA charts respectively to $\{e_t\}$ [25].

2.2 The CUSUM Chart

The basic purpose of a CUSUM chart is to track the distance between the actual data point and the grand mean. Then, by keeping a cumulative sum of these distances, a change in the process mean can be determined, as this sum will continue getting larger or smaller. These cumulative sum statistics are called the upper cumulative sum (C_t^+) and the lower cumulative sum (C_t^-). They are defined by Equation (8) and Equation (9):

$$C_t^+ = \max[0, x_t - (\mu_0 + K) + C_{t-1}^+] \quad (8)$$

$$C_t^- = \max[0, (\mu_0 - K) - x_t + C_{t-1}^+] \quad (9)$$

where μ_0 is the grand mean and K is the slack value which is often chosen about halfway between the target μ_0 and the out-of-control value of the mean μ_1 that we are interested in detecting quickly [1]. So, if the shift is expressed in standard deviation units as $\mu_1 = \mu_0 + \delta\sigma$ (or $\delta = |\mu_1 - \mu_0| / \sigma$), then K is one-half the magnitude of the shift or $K = (\delta\sigma)/2 = (|\mu_1 - \mu_0|)/2$. It is important to select the right value for *K*, since a large value of *K* will allow for large shifts in the mean without detection, whereas a small value of *K* will increase the frequency of false alarms. Normally, *K* is selected to be equal to 0.5σ.

The tabular CUSUM is designed by choosing values for the reference value *K* and the decision interval *H*. Define $K = k\sigma$ and $H = h\sigma$, where σ is the standard deviation of the sample variable used in forming the CUSUM. Using *h*=4 or *h*=5 and *k*=1/2 will generally provide a CUSUM that has good ARL properties against a shift about 1 σ in the process mean [1].

For CUSUM residual chart, the residuals are calculated using Equation (7) where e_t shows normal distribution with mean zero and with constant variance. Then, conventional CUSUM control chart can be applied to the residuals using the formulas given in Equation (8) and Equation (9).

2.3 The EWMA chart

Like CUSUM chart, EWMA is suitable for detecting small process shifts. EWMA chart uses smoothing constant. The smoothing constant λ is that $0<\lambda\leq 1$ [31]. The EWMA is a statistic for monitoring the process that averages the data in a way that gives less and less weight to data as they are further removed in time.

By the choice of weighting factor λ, the EWMA control procedure can be made sensitive to a small or gradual drift in the process. The statistic that is calculated is [1]:

$$z_t = \lambda x_t + (1-\lambda) z_{t-1} \quad (10)$$

where z_t is the moving average at time *t*.

The value of λ can be between zero and one, but it must often chosen between 0.05 and 0.3. The initial value of *z* (i.e. z_0) is set to the grand mean (μ_0) [1]. If the observations x_t are independent random variables with variance σ^2, then the variance of z_t will be

$$\sigma_{z_t}^2 = \sigma^2 \left(\frac{\lambda}{2-\lambda}\right)\left[1-(1-\lambda)^{2t}\right] \quad (11)$$

Therefore the EWMA control chart would be constructed by plotting z_t versus the time *t* (or sample number). The center line and control limits for the EWMA control chart are as follows:

$$UCL = \mu_0 + L\sigma\sqrt{\frac{\lambda}{(2-\lambda)}[1-(1-\lambda)^{2t}]} \quad (12)$$

$$CL = \mu_0 \quad (13)$$

$$LCL = \mu_0 - L\sigma\sqrt{\frac{\lambda}{(2-\lambda)}[1-(1-\lambda)^{2t}]} \quad (14)$$

where *L* is the number of standard deviations from the center-line (width of the control limits). Lucas and Saccucci [32] give tables that help the user to select λ.

2.4 The GMA chart

The GMA chart is used by the purpose of detecting shifts in mean of the process quality data. GMA is a weighted average of all the prior observations (sample mean if using rational sub grouping, with sample sizes greater than one) on a process. The GMA chart is well-suited for the purpose of early detection of small shifts, simply by setting the smoothing constant to smaller values. The statistics plotted on the GMA control chart, when it is used to monitor sample averages, is given in Equation (10). In order to use (10) for tracking the average value of the real time residuals, the estimated average of the real-time residuals for the first window is replaced with process observations. The estimate of the standard deviation of the statistic plotted on the chart is simply $\bar{R}/d_2$, *L* is the width of the control limits, in units of standard deviations of the statistic we plot on the chart. The control limits for the GMA are

$$UCL = \bar{e} + L(\bar{R}/d_2)\left[\lambda/(2-\lambda)\right]^{1/2} \quad (15)$$

$$LCL = \bar{e} - L(\bar{R}/d_2)\left[\lambda/(2-\lambda)\right]^{1/2} \quad (16)$$

where $\bar{e}$ is the center line for the chart [33].

2.5 Computation of the Average Run Lengths (ARLs)

The ARL of the Shewhart charts can be found from:

$$ARL = (1/p) \quad (17)$$

where *p* is the probability of exceeding the control limits by any sample point. Thus, if the process is in control ARL_0= (1 / α) where α is the probability of type I error, but if it is out of control, ARL_1 = (1 / (1 - β)). The probability of not detecting this shift on the first subsequent sample or the β risk is

$$\beta = \Phi\left[\frac{UCL-(\mu_0+k\sigma)}{\sigma/\sqrt{n}}\right] - \Phi\left[\frac{LCL-(\mu_0+k\sigma)}{\sigma/\sqrt{n}}\right] \quad (18)$$

where Φ denotes the standard normal cumulative distribution function [1].

Several techniques can be used to calculate the ARL of a CUSUM. For a one sided CUSUM (that is, C_t^+ or C_t^-) with parameters *h* and *k*, Siegmund's approximation is

$$ARL = \frac{\exp(-2\Delta b) + 2\Delta b - 1}{2\Delta^2} \quad (19)$$

for $\Delta \neq 0$, where $\Delta = \delta^* - k$ for the upper one-sided CUSUM C_t^+, $\Delta = \delta^* - k$ for the lower one-sided CUSUM C_t^-, $b = h + 1.166$, and $\delta^* = (\mu_1 - \mu_0)/\sigma$. If $\Delta = 0$, one can use $ARL = b^2$. The quantity δ^* represents the shift in the mean, in the units of σ, for which the ARL is to be calculated. Therefore, if $\delta^* = 0$, we would calculate ARL_0 from Equation (19), while if $\delta^* \neq 0$, we would calculate the value of ARL_1 corresponding to a shift of size δ^*. To obtain the ARL of two-sided CUSUM from the ARLs of the two one-sided statistics, say ARL^+ and ARL^-, the following formula given in Equation (20) is used [1].

$$\frac{1}{ARL} = \frac{1}{ARL^{+}} + \frac{1}{ARL^{-}} \quad (20)$$

There are two main approaches for computing ARL for an EWMA sequence. The first approach is based on the fact that ARL must satisfy the Fredholm integral equation (see [34]). The second approach is based on the flexible and relatively easy to use Markov chain approach, originally proposed by Brook and Evans in 1972 [35]. We used second approach to calculate the ARLs of EWMA and GMA control schemes. This procedure involves dividing the interval between LCL and UCL into $p = 2m+1$ subintervals of width 2δ, where $\delta = (UCL - LCL)/(2p)$. When the number of subintervals *p* is sufficiently large the finite approach provides an effective method that allows ARL to be effectively evaluated. The EWMA statistic (z_t) is said to be in transient state *j* at time *t* if $H_j - \delta < z_t < H_j + \delta$ for $j = -m,...,-1,0,+1,...,+m$ where H_j represents the midpoint of the *j*th subinterval. The EWMA statistic is in the absorbing state if $z_t \notin [LCL, UCL]$. An approximation for ARL is given by

$$ARL \simeq d^T Q g \quad (21)$$

where *d* is the (*p*, 1) initial probability vector, $Q = (I-P)^{-1}$ is the fundamental (*p*, *p*) matrix, *P* is the (*p*, *p*) transition-probabilities matrix and *g*=*I* is a (*p*, 1) vector of 1s. The initial probability vector *d* contains the probabilities that the statistic z_t starts in a given state. The transition probability matrix *P* contains the one-step transition probabilities. The generic element p_{ij} of *P* represents the probability that the statistic z_t goes from state *i* to state *j* in one step. This probability can be calculated by

$$p_{ij} = \Phi\left(\frac{H_j + \delta - (1-\lambda)H_i}{\lambda}\right) - \Phi\left(\frac{H_j - \delta - (1-\lambda)H_i}{\lambda}\right) \quad (22)$$

3. THE PROCESS MODEL

An autoregressive process of lag 1, AR(1), is the representative model for autocorrelated processes. In an AR(1) process, the current observation is correlated with its previous observation. Past studies emphasize the role of AR(1) processes in process control [36]. An AR(1) model can be expressed as follows:

$$x_t = \xi + \phi x_{t-1} + \varepsilon_t \quad (23)$$

where *t* is the time of sampling, x_t is the sample value at time *t*, ξ is the constant, ϕ is the autoregressive coefficient $(-1 < \phi < 1)$, and ε_t is the independent random error term (common cause variation) at time *t* following $N(0, \sigma_\varepsilon^2)$. Let X_t with an increasing linear trend (trend AR(1) process) is represented by:

$$X_t = x_t + dt \quad (24)$$

where *d* is the trend slope in terms of *t*, and X_t with a shift or jump is given by:

$$Z_t = X_t + \delta_\mu \quad (25)$$

where δ_μ is the magnitude of upward mean shift. In this study, our aim is to compare the performances of residual charts for an upward shift in the mean of $\{Z_t\}$. ARL measure is used for comparison.

To illustrate how these charts signal, we easily computerized design procedures of the charts with MATLAB 7.4.0, and applied them to a sample of *N*=500 observations generated by using Equation (25). Design of the charts for this sample data was completed in less than 1s of CPU time on a personal computer (AMD turion, 1.79 GHZ, 2.87 GB Ram). To model assignable causes, a sustained shift of magnitude δ_μ is induced in the mean of Z_t in Equation (25) starting at the initial start-up of the system.

4. COMPARISON OF CONTROL CHARTS FOR RESIDUALS

In this article, we will compare the performances of Shewhart individual chart for residuals, Shewhart $\bar{x}$ and *R* chart for residuals, CUSUM residual, EWMA residual, and GMA residual control charts for trend AR(1) process for a wide range of possible shifts and autocorrelation coefficients. At the rest of the paper, we will use Shewhart individual chart, Shewhart $\bar{x}$ and *R* chart, CUSUM chart, EWMA chart, and GMA chart expressions for short, to represent these charts for residuals. In this section, we evaluate ARL performances of the charts using the following design parameters: $\xi = 0$, $x_1 = 10$, $\varepsilon \sim N(0,1)$, *N*=500, and *d*=0.2. To investigate the performance, we generated data sets using Equation (25), and employed a wide range of possible shifts and autocorrelation coefficients. Each data set involves 500 observations. The considered shift magnitudes (in the unit of σ_e) and autocorrelation coefficients are δ_μ = 0.0, 0.5, 1.0, 1.5, 2.0, 2.5, 3.0, and $\phi = \mp 0.95$, ∓ 0.75, ∓ 0.475, ∓ 0.25, 0, respectively. For the sake of simplicity, we classified shift magnitudes in three groups as small ($\delta_\mu = 0.5\sigma_e$, $1.0\sigma_e$), moderate ($\delta_\mu = 1.5\sigma_e$, $2.0\sigma_e$), large ($\delta_\mu = 2.5\sigma_e$, $3.0\sigma_e$), and autocorrelation coefficients as weak ($\phi = \mp 0.25$), moderate ($\phi = \mp 0.475$, ∓ 0.75) and strong ($\phi = \mp 0.95$). For each case considered, 1000 independent replications were performed. ARL calculations are performed by using the formulas given in Section 2.5 through process observations obtained by simulation experiments. Simulation results are explained in detail below.

The ARLs for the EWMA chart and GMA chart with $\lambda = 0.05$ are obtained from process observations through simulations for step mean shifts of 0.0, 0.5, 1.0, 1.5, 2.0, 2.5, 3.0 in the unit of σ_e, where σ_e is the standard deviation of $\{e_t\}$. For the Shewhart, EWMA and GMA charts, the control limits $L\sigma$ are adjusted to have the in-control ARL close to 370, which corresponds to the in-control ARL of the 3-sigma Shewhart chart applied to an *iid* sequence with a normal distribution. For the EWMA and GMA charts *L*=2.5 is chosen for $\lambda = 0.05$ to have the in-control ARL close to 370 [32]. For the Shewhart chart *L*=3 is chosen to have the in-control ARL close to 370 [1]. For the CUSUM chart, k and h are set to 0.5 and 4.77, respectively, to have the in-control ARL close to 370 for $\phi = \mp 0.95, \mp 0.75, \mp 0.475, \mp 0.25, 0$. Hawkins [37] gives tables to select k and h for Two-Sided Tabular CUSUM chart to have in-control ARL close to 370. The ARL values of these residual charts for trend AR(1) process were calculated by using the formulations given in Section (2.5) through process observations obtained from simulation experiments. The ARL values are listed in Table 1 for $\phi \geq 0$ and Table 2 for $\phi < 0$. To investigate the performance of the residual charts for stationary AR(1) process, we generated data sets using Equation (25) with design parameter d=0. ARL values of the residual charts for stationary AR(1) process are also calculated by using the formulations given in Section (2.5) through simulation experiments, and results are listed in Table 1 and Table 2 in parenthesis. The comparison mechanism is displayed in Figure 1.

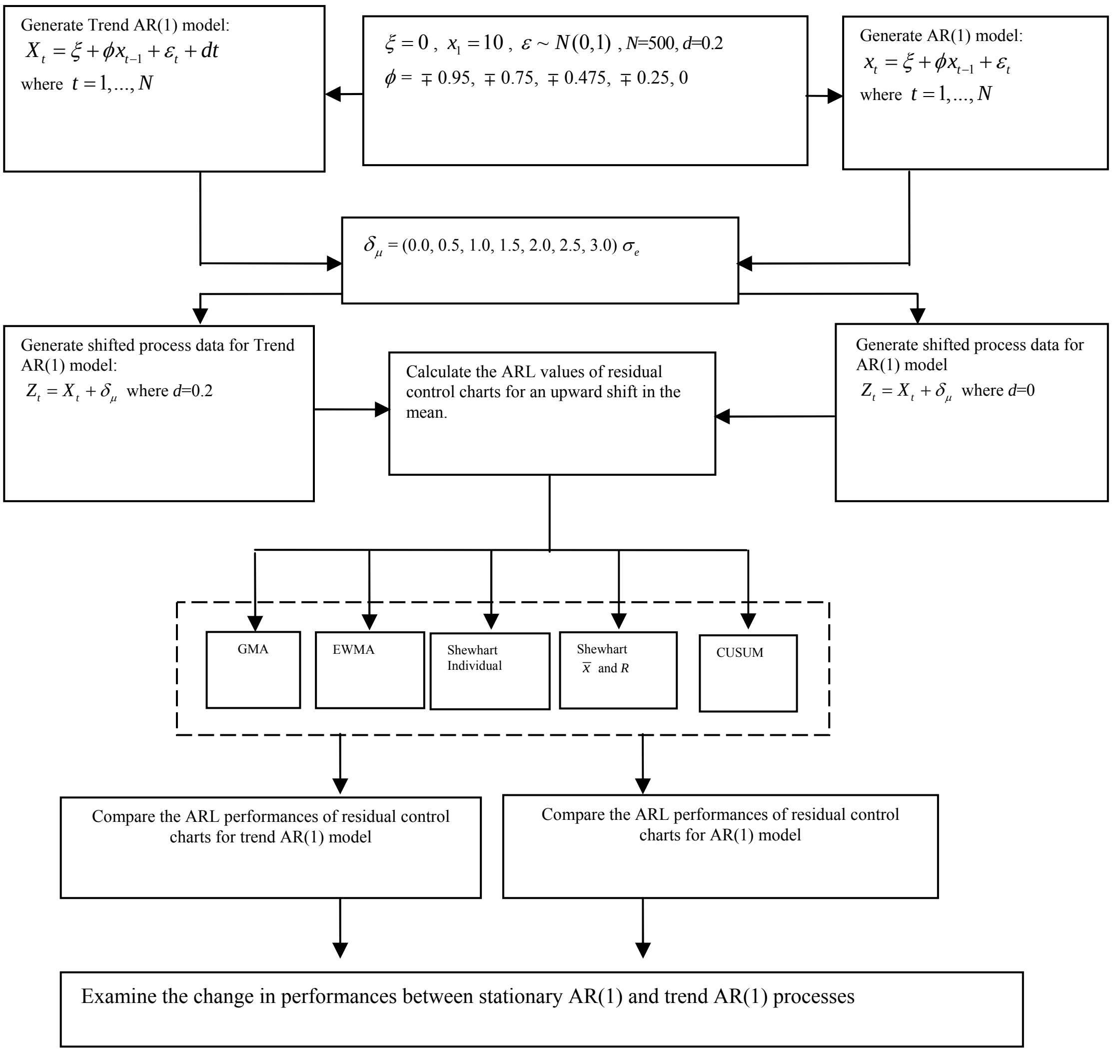

Figure 1. Comparison mechanism.

Table 1. ARLs for trend AR(1) and AR(1) processes ($\phi \geq 0$)

ϕ	Mean Shift	GMA	EWMA	Shewhart Individual	Shewhart $\bar{x}$ and R	CUSUM
0.95	0.0	390.175 (365.001)	343.951 (376.312)	370.445 (370.445)	370.445 (370.445)	371.482 (370.481)
	0.5	264.952 (271.680)	230.328 (253.694)	357.949 (357.420)	335.857 (334.756)	308.136 (308.013)
	1.0	140.454 (128.373)	124.045 (117.552)	324.896 (323.111)	260.194 (259.183)	200.186 (200.016)
	1.5	80.244 (73.883)	70.682 (59.056)	279.589 (270.628)	185.196 (185.180)	122.406 (122.346)
	2.0	51.449 (48.308)	46.661 (48.891)	234.103 (230.063)	127.854 (126.899)	76.800 (76.671)
	2.5	35.908 (23.677)	34.219 (35.111)	191.249 (186.769)	88.079 (88.051)	50.781 (49.991)
	3.0	28.186 (21.131)	26.386 (26.986)	154.430 (150.040)	61.286 (61.272)	35.544 (34.864)
0.75	0.0	390.170 (390.156)	324.999 (359.322)	370.445 (370.445)	370.445 (370.445)	371.482 (371.322)
	0.5	124.825 (115.326)	102.705 (104.579)	313.045 (315.144)	237.385 (237.494)	173.908 (173.711)
	1.0	44.624 (42.356)	37.783 (38.183)	208.912 (213.183)	103.132 (102.193)	60.122 (60.022)
	1.5	23.988 (23.180)	22.655 (22.901)	128.255 (132.516)	45.392 (45.311)	27.276 (26.132)
	2.0	16.312 (16.120)	15.439 (15.692)	78.282 (81.690)	21.762 (20.982)	15.811 (14.122)
	2.5	12.479 (11.991)	11.695 (11.576)	44.234 (46.804)	11.439 (10.946)	10.758 (10.159)
	3.0	9.786 (9.628)	9.245 (9.261)	31.323 (33.156)	6.582 (6.171)	8.072 (7.692)
0.475	0.0	390.170 (365.001)	363.200 (376.312)	370.445 (370.445)	370.445 (370.445)	371.482 (370.220)
	0.5	57.624 (41.341)	54.594 (57.336)	252.661 (248.930)	148.750 (147.983)	92.216 (92.116)
	1.0	22.060 (20.806)	21.149 (22.873)	119.302 (115.080)	40.651 (39.961)	24.893 (24.293)
	1.5	12.969 (12.313)	12.442 (12.394)	55.644 (52.834)	13.607 (13.537)	11.859 (11.359)
	2.0	9.168 (8.741)	8.743 (8.794)	27.726 (26.051)	5.707 (4.893)	7.525 (6.945)
	2.5	7.057 (6.800)	6.891 (6.839)	14.915 (13.918)	2.956 (2.343)	5.480 (4.886)
	3.0	5.803 (5.588)	5.601 (5.619)	8.662 (8.056)	1.853 (1.652)	4.303 (3.902)
0.25	0.0	390.173 (390.156)	349.604 (359.322)	370.445 (370.445)	370.445 (370.445)	371.482 (369.883)
	0.5	43.747 (40.716)	38.267 (37.378)	205.192 (209.490)	99.811 (98.976)	58.005 (57.935)
	1.0	16.120 (15.213)	15.009 (15.253)	75.421 (78.755)	20.644 (20.342)	15.277 (14.822)
	1.5	9.600 (9.401)	9.034 (9.003)	29.817 (31.581)	6.210 (6.112)	7.843 (7.443)
	2.0	6.893 (6.779)	6.620 (6.610)	13.388 (14.293)	2.671 (2.321)	5.213 (5.011)
	2.5	5.438 (5.336)	5.226 (5.225)	6.833 (7.315)	1.571 (1.172)	3.897 (3.342)
	3.0	4.551 (4.468)	4.329 (4.338)	3.941 (4.211)	1.182 (1.173)	3.110 (3.012)
0.0	0.0	390.170 (365.001)	368.792 (376.312)	370.445 (370.445)	370.445 (370.445)	371.482 (370.882)
	0.5	28.124 (28.998)	26.636 (26.885)	153.893 (149.511)	60.959 (60.732)	35.358 (35.325)
	1.0	11.284 (10.782)	10.798 (10.852)	38.816 (41.028)	9.824 (9.123)	9.909 (9.899)
	1.5	7.058 (6.771)	6.854 (6.810)	14.747 (13.761)	2.924 (2.314)	5.451 (5.432)
	2.0	5.108 (4.986)	4.995 (5.013)	6.210 (5.774)	1.479 (1.453)	3.744 (3.721)
	2.5	4.137 (3.984)	4.016 (4.005)	3.198 (2.988)	1.103 (1.102)	2.850 (2.834)
	3.0	3.489 (3.350)	3.382 (3.431)	1.978 (1.869)	1.015 (1.011)	2.300 (2.213)

For trend AR(1) process, as can be seen in Table 1, it is clear that when process exhibit weak positive autocorrelation the EWMA and GMA charts perform equally well for small shifts while CUSUM and Shewhart $\bar{X}$ and R perform better for moderate to large shift. For moderate positive autocorrelation, EWMA and GMA charts perform almost the same and better than other charts for small mean shifts, while they perform similar with CUSUM chart for moderate shifts. For large shifts, CUSUM and Shewhart $\bar{x}$ and R charts perform better. When a strong positive autocorrelation exist in process data, the EWMA and GMA charts perform better than other charts for small to large mean shifts while the EWMA, GMA and the CUSUM charts perform better than the Shewhart type control charts for large shifts. Shewhart individual chart performs worst for strong positive autocorrelation and Shewhart $\bar{x}$ and R chart performs well when it is compared with Shewhart individual chart. It must be noted that the performance of CUSUM, EWMA and GMA charts are almost the same and these charts perform better than the Shewhart type charts in detecting small shifts for $\phi > 0$. Overall performance of the Shewhart individual chart is not good.

Table 2. ARLs for trend AR(1) and AR(1) processes ($\phi < 0$)

ϕ	Mean Shift	GMA	EWMA	Shewhart Individual	Shewhart $\bar{x}$ and R	CUSUM
-0.25	0.0	390.177 (390.156)	349.623 (359.322)	370.445 (370.445)	370.445 (370.445)	371.482 (371.482)
	0.5	20.186 (19.398)	19.326 (19.475)	105.422 (109.389)	33.628 (33.513)	21.474 (21.371)
	1.0	8.558 (8.435)	8.098 (8.097)	22.567 (23.980)	4.528 (3.928)	6.729 (6.526)
	1.5	5.465 (5.334)	5.232 (5.210)	6.855 (7.339)	1.574 (1.264)	3.902 (3.552)
	2.0	4.089 (3.997)	3.873 (3.885)	2.921 (3.110)	1.077 (1.056)	2.744 (2.732)
	2.5	3.298 (3.239)	3.141 (3.154)	1.679 (1.762)	1.005 (1.004)	2.115 (2.105)
	3.0	2.802 (2.748)	2.672 (2.672)	1.230 (1.267)	1.000 (1.000)	1.720 (1.687)
-0.475	0.0	390.170 (365.001)	363.958 (376.312)	370.445 (370.445)	370.445 (370.445)	371.482 (371.474)
	0.5	14.217 (14.730)	13.648 (13.492)	64.389 (61.304)	16.584 (15.896)	13.323 (13.122)
	1.0	6.301 (6.007)	6.056 (6.041)	10.637 (9.903)	2.182 (2.072)	4.702 (4.612)
	1.5	4.123 (3.965)	4.003 (3.986)	3.152 (2.946)	1.098 (1.079)	2.833 (2.723)
	2.0	3.136 (3.032)	3.051 (3.046)	1.557 (1.486)	1.003 (1.002)	2.026 (2.011)
	2.5	2.553 (2.454)	2.468 (2.467)	1.129 (1.105)	1.000 (1.000)	1.576 (1.569)
	3.0	2.141 (2.091)	2.107 (2.097)	1.021 (1.015)	1.000 (1.000)	1.290 (1.289)
-0.75	0.0	390.172 (390.156)	344.842 (359.322)	370.445 (370.445)	370.445 (370.445)	371.482 (371.384)
	0.5	8.270 (8.084)	7.898 (7.879)	21.125 (22.465)	4.216 (4.187)	6.502 (6.401)
	1.0	3.982 (3.921)	3.785 (3.767)	2.734 (2.908)	1.062 (1.059)	2.667 (2.363)
	1.5	2.738 (2.686)	2.562 (2.560)	1.194 (1.227)	1.000 (1.000)	1.675 (1.545)
	2.0	2.091 (2.076)	2.048 (2.047)	1.011 (1.015)	1.000 (1.000)	1.221 (1.112)
	2.5	1.989 (1.946)	1.929 (1.929)	1.000 (1.000)	1.000 (1.000)	1.000 (1.000)
	3.0	1.690 (1.627)	1.537 (1.537)	1.000 (1.000)	1.000 (1.000)	1.000 (1.000)
-0.95	0.0	390.170 (365.001)	368.285 (376.312)	370.445 (370.445)	370.445 (370.445)	371.482 (371.482)
	0.5	3.356 (3.312)	3.261 (3.329)	1.808 (1.714)	1.008 (1.005)	2.198 (2.088)
	1.0	1.998 (1.962)	1.964 (1.966)	1.001 (1.000)	1.000 (1.000)	1.021 (1.035)
	1.5	1.146 (1.081)	1.090 (1.088)	1.000 (1.000)	1.000 (1.000)	1.000 (1.000)
	2.0	1.000 (1.000)	1.000 (1.000)	1.000 (1.000)	1.000 (1.000)	1.000 (1.000)
	2.5	1.000 (1.000)	1.000 (1.000)	1.000 (1.000)	1.000 (1.000)	1.000 (1.000)
	3.0	1.000 (1.000)	1.000 (1.000)	1.000 (1.000)	1.000 (1.000)	1.000 (1.000)

From Table 2 we observe that, for small shifts, the Shewhart individual chart is the worst performer for weak and moderate negative autocorrelation. For large mean shifts, all charts perform well. For weak autocorrelation and for small shifts, the EWMA, GMA and CUSUM charts are the best performers. CUSUM and Shewhart type charts perform equally well for moderate to strong autocorrelation. For small shifts, overall performance of the residual charts, except Shewhart individual chart, is good. For strong negative autocorrelation, the Shewhart chart performs little better than the all. Overall performance of the Shewhart type charts and CUSUM chart for negative autocorrelation are little better than the all for moderate to large shifts. It is well known that negative autocorrelation does not affect ARL_0 performance badly and the results given in Table 1 and Table 2 support this statement. For each autocorrelation-shift combination, the best performed charts are given in Tables 3-4 in a descending order of ARL performance.

Table 3. Best performed control charts for trend AR (1) process ($\phi \geq 0$)

ϕ / δ_μ	Strong Positive	Moderate Positive	Weak Positive	Uncorrelated
Small	EWMA GMA	EWMA GMA	EWMA GMA	EWMA GMA CUSUM
Moderate	EWMA GMA	CUSUM Shewhart $\bar{x}$ and R	Shewhart $\bar{x}$ and R CUSUM	Shewhart $\bar{x}$ and R
Large	EWMA GMA CUSUM	Shewhart $\bar{x}$ and R CUSUM	Shewhart $\bar{x}$ and R CUSUM	Shewhart $\bar{x}$ and R Shewhart individual

Table 4. Best performed control charts for trend AR (1) process ($\phi < 0$)

ϕ / δ_μ	Strong Negative	Moderate Negative	Weak Negative
Small	Shewhart $\bar{x}$ and R Shewhart individual CUSUM	CUSUM Shewhart $\bar{x}$ and R EWMA GMA	CUSUM EWMA GMA
Moderate	Shewhart $\bar{x}$ and R Shewhart individual CUSUM EWMA GMA	Shewhart $\bar{x}$ and R Shewhart individual CUSUM	Shewhart $\bar{x}$ and R CUSUM
Large	Shewhart $\bar{x}$ and R Shewhart individual CUSUM EWMA GMA	Shewhart $\bar{x}$ and R Shewhart individual CUSUM	Shewhart $\bar{x}$ and R Shewhart individual CUSUM

The comparisons given in Table 3 and Table 4 show that when strong positive autocorrelation exist in trend AR(1) process, EWMA, GMA, and CUSUM charts perform better than the Shewhart individual chart. The Shewhart individual chart performs best in case of negative autocorrelation for large shifts. On the contrary, in case of small and moderate shifts, Shewhart individual chart performs worst for positive autocorrelation. The comparison also shows that the CUSUM, EWMA and GMA charts perform almost similar.

On the other hand, if we examine the change in performances between stationary AR(1) and trend AR(1) processes, observing Tables 1-2, it is seen that for strong positive autocorrelation while Shewhart $\bar{x}$ and R, and CUSUM charts keep their performances, GMA, EWMA and Shewhart individual charts perform worse in trend AR(1) process. For small shifts and moderate positive autocorrelation for trend AR(1) process, while Shewhart individual and EWMA charts perform better, GMA chart performs worse compared to their performance in AR(1) process. For weak positive autocorrelation and weak negative autocorrelation, Shewhart individual chart performs better for small shifts. For other cases, there are no significant changes at ARL performances.

5. CONCLUSION

A widely accepted strategy for monitoring autocorrelated processes is to use residuals, uncorrelated random variables, of time series. In this study, Shewhart individual, Shewhart $\bar{x}$ and R, EWMA, CUSUM, and GMA charts were applied to residuals of AR(1) and trend AR(1) process, and their ARLs for two type of processes are calculated by using the formulas given in Section (2.5) through simulation experiments. First, sensitivities of the charts to several magnitudes of mean shifts of trend AR(1) process are evaluated. Then, the charts' performances in two processes are compared. The aim was to observe how the performance of the charts are change by addition of an increasing linear trend in AR(1) process. The most conspicuous observations are *i*) for small shifts and moderate positive autocorrelation, Shewhart individual and EWMA charts perform better for trend AR(1) process *ii*) only the Shewhart $\bar{x}$ and R and CUSUM charts' performances are the same for trend AR(1) and AR(1) process. For future research, this study could be extended for autocorrelated data with decreasing trend.

ACKNOWLEDGEMENT

The authors wish to thank the editor and the referees for their thoughtful and detailed suggestions that improved the final version of this paper.

REFERENCES

[1] Montgomery, D. C., Introduction to Statistical Quality Control 3rd ed., John Wiley & Sons Inc., New York, (1997).

[2] Pacella, M. and Semeraro, Q., "Using recurrent neural networks to detect changes in autocorrelated processes for quality monitoring", ***Comp Ind Eng***, 52(4): 502–520, (2007).

[3] Kramer, H. and Schmid, W., "Control charts for time series", ***Nonlinear Anal-Theor***, 30(7): 4007-4016, (1997).

[4] Reynolds, M.R. and Lu, C.W., "Control charts for monitoring processes with autocorrelated data", ***Nonlinear Anal-Theor***, 30(7): 4059-4067, (1997).

[5] Yang, J. and Makis, V., "On the performance of classical control charts applied to process residuals", ***Comput Ind Eng***, 33(1-2): 121-124, (1997).

[6] Zhang, N.F., "Detection capability of residual control chart for stationary process data", ***J Appl Stat***, 24(4), 475-492, (1997).

[7] Lu, C.W. and Reynolds, M.R., "EWMA control charts for monitoring the mean of autocorrelated processes", ***J Qual Technol***, 31(2): 166-188, (1999).

[8] Luceno, A. and Box, G.E.P., "Influence of the sampling interval, decision limit and autocorrelation on the average run length in CUSUM charts", ***J Appl Stat***, 27(2): 177-183, (2000).

[9] Rao, B.V., Disney, R.L. and Pignatiello, J.J., "Uniqueness and converges of solutions to average run length integral equations for cumulative sum and other control charts", ***IEEE T***, 33(6): 463-469, (2001).

[10] Jiang, W., Wu, H., Tsung, F., Nair V. and Tsui, K.L., "PID Charts for Process Monitoring", ***Technometrics***, 44(3): 205-214, (2002).

[11] Kacker, R. and Zhang, N.F., "Online control using integrated moving average model for manufacturing errors", ***Int J Prod Res***, 40(16): 4131-4146, (2002).

[12] Shu, L., Apley, D.W. and Tsung, F., "Autocorrelated process monitoring using triggered cuscore charts", ***Qual Reliab Eng Int***, 18(5): 411-421, (2002).

[13] Ben-Gal, I., Morag, G. and Shmilovici, A., "Context-based statistical process control: A monitoring procedure for state-dependent processes", ***Technometrics***, 45(4): 293-311, (2003).

[14] Snoussi, A., Ghourabi, M.E. and Limam, M., "On spc for short run autocorrelated data", ***Commun Stat-Simul C***, 34(1): 219-234, (2005).

[15] Kim, S.H., Alexopoulos, C., Goldsman, D. and Tsui, K.L., "A new model-free CUSUM procedure for autocorrelated processes", Technical report, School of Industrial and Systems Engineering, Georgia Institute of Technology, Atlanta, GA. Retrieved from http://www2.isye.gatech.edu/~skim/MFC.pdf, (2006).

[16] Noorossana, R. and Vaghefi, S.J.M., "Effect of autocorrelation on performance of the MCUSUM control chart", ***Qual Reliab Eng Int***, 22(2): 191-197, (2006).

[17] Triantafyllopoulos, K., "Multivariate control charts based on Bayesian state space models", ***Qual Reliab Eng Int***, 22(6): 693-707, (2006).

[18] Yang, S.F. and Yang, C.M., "An approach to controlling two dependent process steps with autocorrelated observations", ***Int J Adv Manuf Tech***, 29(1-2): 170-177, (2006).

[19] El Ghourabi, M. and Limam, M., "Residual responses to change patterns of autocorrelated processes", ***J Appl Stat***, 34(7): 785-798, (2007).

[20] Costa, A.F.B. and Claro, F.A.E., "Double sampling $\overline{X}$ control chart for a first-order autoregressive moving average process model", ***Int J Adv Manuf Tech***, 39(5-6): 521-542, (2008).

[21] Zou, C., Wang, Z. and Tsung, F., "Monitoring autocorrelated processes using variable sampling schemes at fixed-times", ***Qual Reliab Eng Int***, 24(1): 55-69, (2008).

[22] Sheu, S.H. and Lu, S.L., "Monitoring the mean of autocorrelated observations with one generally weighted moving average control chart", ***J Stat Comput Sim,*** 79(12): 1393-1406, (2009).

[23] Weiss, C.H. and Testik, M.C., "CUSUM Monitoring of First-Order Integer-Valued Autoregressive Processes of Poisson Counts", ***J Qual Technol***, 41(4): 389-400, (2009).

[24] Knoth, S., Morais, M.C., Pacheco, A. and Schmid, W., "Misleading Signals in Simultaneous Residual Schemes for the Mean and Variance of a Stationary Process", ***Commun Stat-Theor M***, 38(16-17): 2923-2943, (2009).

[25] Zhang, N.F., "Statistical control charts for monitoring the mean of a stationary process", ***J Stat Comput Sim***, 66(3): 249-258, (2000).

[26] Harris, T.J. and Ross, W.H., "Statistical process-control procedures for correlated observations", ***Can J Chem Eng***, 69(1): 48-57, (1991).

[27] Wardell, D.G., Moskowitz, H. and Plante, R.D., "Run-length distribution of special-cause control charts for correlated processes", ***Technometrics***, 36(1): 3-7, (1994).

[28] Zhang, N.F., "A statistical control chart for stationary process data", ***Technometrics***, 40(1): 24-38, (1998).

[29] Itoh, T., Saito, H., Takumi, Y. and Shimizu, T., "Process analysis techniques for cement kilns", ***IEEE Transactions on Industry and General Applications***, 7(4): 470-479, (1971).

[30] Nouros, P.G., Georgiou, C.A. and Polissiou, M.G., "Direct parallel flow injection multichannel spectrophotometric determination of olive oil peroxide value", ***Anal Chim ACTA***, 389(1-3): 239-245, (1999).

[31] Shu, L., Tsung, F. and Tsui, K. L., "Effects of estimation errors on cause-selecting charts", ***IEEE T.***, 37(3): 559-567, (2005).

[32] Lucas, J. and Saccucci, M.S., "Exponentially weighted moving average control schemes, properties and enhancements", ***Technometrics***, 32(1): 1-12, (1990).

[33] Yourstone, S.A. and Montgomery, D.C., "A time-series approach to discrete real-time process quality control", ***Qual Reliab Eng Int***, 5(4): 309-317, (1989).

[34] Crowder, S.V., "A simple method for studying run-length distributions of exponentially weighted moving average charts", ***Technometrics***, 29(4): 401-407, (1987).

[35] Pham, H., Springer Handbook of Engineering Statistics 1st ed., Springer, New Jersey, (2006).

[36] Guh, R.S., "Real-time recognition of control chart patterns in autocorrelated processes using a learning vector quantization network-based approach", ***Int J Prod Res***, 46(14): 3959-3991, (2008).

[37] Hawkins, D.M., "Cumulative sum control charting: an underutilized SPC tool", ***Qual Eng***, 5(3): 463-477, (1993).